CF$_2$-bridged C$_{60}$ dimers and their optical transitions

Panagiotis Dallas *[a], Shen Zhou [a], Stuart Cornes [a], Hiroyuki Niwa [b], Yusuke Nakanishi [b], Yasuhiro Kino [b], Tim Puchtler [c], Robert.A.Taylor [c], G.Andrew.D.Briggs [a], Hisanori Shinohara *[b] and Kyriakos Porfyrakis *[a]

Fullerene dyads bridged with perfluorinated linking groups have been synthesized through a modified arc-discharge procedure. The addition of Teflon inside an arc-discharge reactor leads to the formation of dyads, consisting of two C$_{60}$ fullerenes bridged by –CF$_2$-groups. The bridging groups consisting of electronegative atoms, lead to different energy levels and to new features in the photoluminescence spectrum. A suppression of the singlet oxygen photosensitization, indicated that the radiative decay from singlet to singlet state is favoured against the intersystem crossing singlet to triplet transition.

Fullerene dimers [1] have been synthesized by utilizing various bridging groups that link the two buckyballs. A wide range of methods can be found in the literature, with examples including the dimerization of pristine C$_{60}$ [2] through high pressure treatment, mechanochemical synthesis using KCN and K$_2$CO$_3$ [3] or dipolar cycloaddition reactions. [4] Besides the [2+2] carbon linking between the two buckyballs, typical bridging groups include oxygen [5] and methylene units, as well as photo-switchable azobenzenes. [6] A dimerization of adjacent fullerenes inside carbon nanotube peapods occurs as well. A fullerene dimerization was monitored and distinguished between formations of dyads in the first stage with small nanotubes to be formed in subsequent stages through bond fusion. [7] Fullerene dimers provide a class of materials for applications in artificial photosynthesis and molecular electronic devices due to their richer energy level structure compared to the single cage fullerene counterparts. [8] Despite the number of fullerene dimers presented in the literature, the synthesis of -CF$_n$- bridged dimers has not been reported due to difficulties arising from the poor reactivity of the C-F bond. We achieved the synthesis of this unexpected dyad in the high temperature plasma conditions of an arc-discharge reactor by evaporating Teflon simultaneously with graphite. We also demonstrated their reactivity with a Bingel-Hirsch reaction. The fluorine addition could be beneficial in terms of optoelectronic

[a] Dr.P.Dallas, Mr.S.Zhou, Dr.S.Cornes, Prof.G.A.D.Briggs, Prof.K.Porfyrakis
Department of Materials, University of Oxford
Oxford OX1 3PH, United Kingdom
E-mail: panagiotis.dallas@materials.ox.ac.uk;
kyriakos.porfyrakis@materials.ox.ac.uk
[b] Mr.H.Niwa, Dr.Y.Nakanishi, Mr.Y.Kino, Prof.Hisanori Shinohara
Department of Chemistry
Nagoya University, Japan
E-mail: noris@nagoya-u.jp
[c] Dr.T.Puchtler, Prof.R.A.Taylor
Department of Physics
Clarendon Laboratory, University of Oxford, United Kingdom

applications since it has been demonstrated that the presence of the highly electronegative fluorine atoms in conjugated polymers leads to high-performing materials for field-effect transistors with a bright blue photoluminescence. [9]
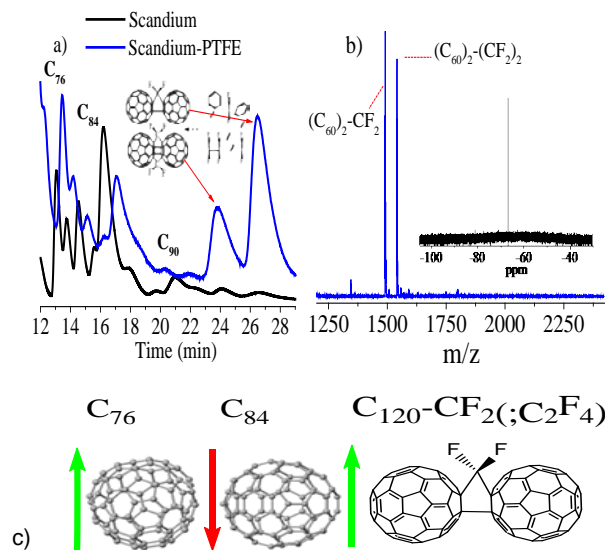

Figure 1. a) HPLC traces of fullerene extract from scandium rods, without (black) and with (blue), Teflon and the proposed structure of the dyads (inset). b) MALDI-TOF analysis indicating the two systems and various other perfluorinated fullerenes with –CF$_3$ and/or –CF$_2$ groups. ^{19}F NMR as inset. c) Fullerene monomers and dyad. Red arrow indicates a decrease in the yield and a green an increase after the addition of Teflon.

A modified arc-discharge procedure was used to synthesize the dyads. [10] Our initial target was the synthesis of perfluorinated empty cages and endohedral metallofullerenes. The decomposition of Teflon close to the arc resulted in reactive CF$_{2n}$ and C$_{2n}$ fragments as precursor molecules. Addition of the -CF$_2$-on the fullerene cage results to perfluorinated empty cages and metallofullerenes, and surprisingly, to the formation of the unusual -CF$_2$- bridged dimers, isolated through HPLC (Fig.1 and S1). By integrating the HPLC peaks, we calculated the following yields: C$_{60}$: 72.94 %, C$_{70}$: 24.41 %, C$_{76-78}$: 0.63 %, C$_{84}$: 0.39 %, C$_{90}$: 0.1 %, (C$_{60}$)$_2$-(CF$_2$)$_2$: 0.29 %, (C$_{60}$)$_2$-CF$_2$: 1.25 %. Our first analysis on elucidating the structure of the dimers was based on detailed mass spectrometry (Fig. S2). We observed two unique structures with an m/z=1541 (HPLC retention time 24-26 min), and an m/z=1491 (HPLC retention time 27-29 min), while the yield of C$_{84}$ and metallofullerenes was suppressed after the addition of Teflon (Fig.1). We assigned the two dyads as C$_{60}$-(CF$_2$)$_2$-C$_{60}$ and

C_{60}-CF_2-C_{60}. In the mass spec of the C_{60}-CF_2-C_{60} we distinguished two fragments, the C_{60}-CF_2 and C_{60} at m/z=771 and m/z=720, respectively. The C_{60}-$(CF_2)_2$-C_{60} dimer is not subject to fragmentation. We suspect this is due to the rigid structure of its bridge consisting of two linking CF_2 groups. The m/z=50 difference between the dyads, hints to the presence of CF_2-groups. The presence of fluorine is further confirmed by NMR spectroscopy with the ^{19}F NMR spectra providing evidence for the presence of fluorine atoms, (Fig. S3a). The $(C_{60})_2$-CF_2 dyads is showing a peak located at -67.04 ppm. [11] As a comparison, the ^{19}F spectrum of $(C_{60})_2$-$(CF_2)_2$ presents two peaks at -67 ppm and -66.55 ppm, due to different environment of the fluorine atoms with respect to the carbon cage. The ^{13}C NMR is shown in Fig. S4b. The spectrum for the $(C_{60})_2$-$(CF_2)_2$, demonstrates weak signals for fullerene sp^2 carbons, seen in the expected region for a C_{60} dimer, 140-152 ppm. [12] A signal for sp^3 carbon environment was also seen at 29.1 ppm. The signal for the sp^3 CF_2 carbon was not observed as it was obscured by residual solvent peaks. The FTIR spectra (Fig. S3c) provide a strong indication on the presence of perfluorinated groups from the appearance of the very strong antisymmetric and symmetric C-F vibration fingerprint peaks at 1092 and 1031 cm^{-1} in both samples. Fig. S3d-f also shows the Raman spectra of C_{60} and of the two dyads revealing the presence of all eight vibration modes. The symmetry groups representing them are given above each peak. The $A_g(1)$ represents an in and out of plane vibration and while it is quite strong in the pristine C_{60}, it nearly disappears in both dyads. The $H_g(8)$ hexagon shear mode [13] appears with increased intensity in the dimers. The pentagonal pinch $A_g(2)$ and the pentagon shear mode, assigned to the isolated pentagon ring, both remain sharp and relatively strong in all samples with a blue shift in the dyads compared to pristine fullerene, something expected for polymerized or functionalized C_{60}. The five-fold degenerate, $H_g(1)$ mode shifts from 33.4 meV (269 cm^{-1}) for pristine C_{60} to 30.5 meV (246 cm^{-1}) for the dyads. Due to change of symmetry, a peak appears at 15 meV (122 cm^{-1}). These low energy features originate from inter-ball vibrational modes. In previous studies on C_{120}, two peaks at 127 and 139 cm^{-1} were observed, in relative agreement with the work herein. [13] The materials exhibit a limited reactivity with Lewis acids such as $TiCl_4$, something that is indicating that the oxidation potentials are expected to be close to the threshold of 0.62-0.72 V vs Fc/Fc^+. [14] The mass spectra after the Lewis acid reaction are shown in Fig. S4. Since the surface functionalization of fullerenes is a necessary step for their utilization in various applications, the reactivity of the dimers was tested through a Bingel-Hirsch reaction. The MALDI-TOF analysis revealed the presence of mono-, bis-, tris-, tetra-, and penta-malonate adducts. All peaks were separated by m/z=158, the value assigned to each malonate (Fig.2). A more careful analysis of the mass spectrum reveals fragments at m/z=878 and m/z=1036 of the mono- and bis-adducts of C_{60}.
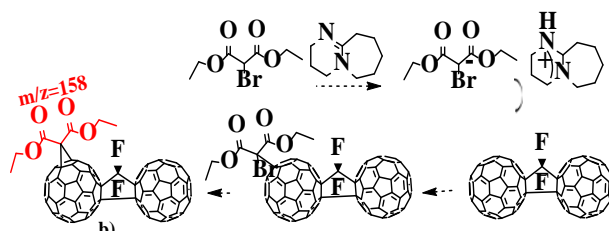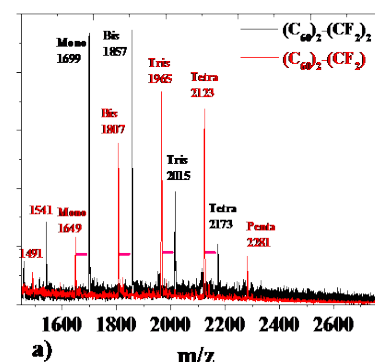

Figure 2. a,b) Schematic representation of the Bingel reaction and mass spectra of the malonate derivatives.

The cyclopropane derivatives were isolated through HPLC (Fig.S5) and their UV-Visible spectra are presented in Fig.3f in comparison with parent, pristine dyads. The absorbance UV-vis spectra (Fig. 3) were recorded in both toluene and CS_2 and the dyad with one -CF_2- group resembles the pristine C_{60} more, with very weak absorbance peaks at 540, 605 and 688 nm. In contrast, the dimer with two bridging -CF_2- groups has a featureless spectrum without any pronounced absorbance peaks except a shoulder at 428 nm, a fingerprint absorbance for functionalized C_{60}. We then studied the fluorescence of the samples, since the light emitting properties of fullerenes are important for biomedical applications or even for potential readout schemes of quantum information processing architectures. [15]
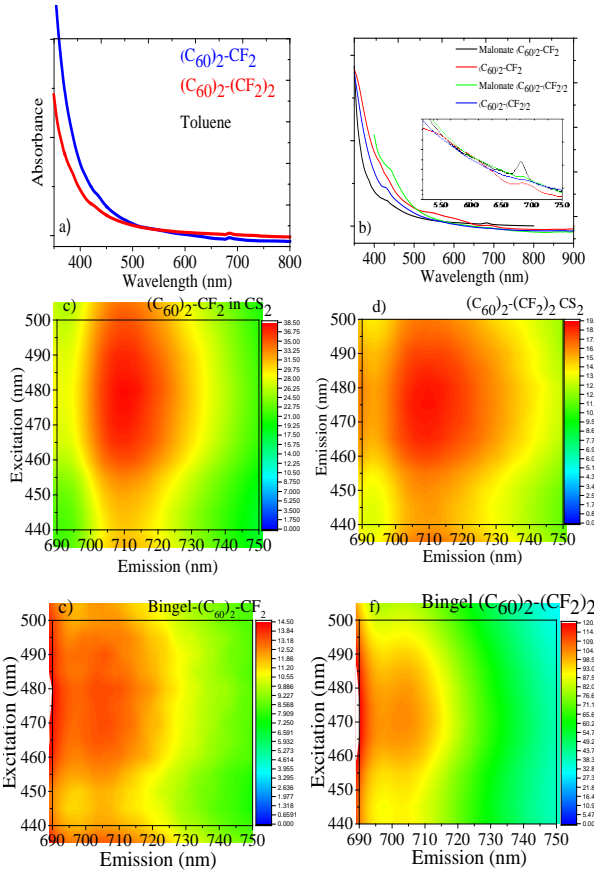
Figure 3. a) UV-Visible spectra recorded in toluene b) UV-visible spectra for the dyads and their Bingel derivatives recorded in CS2 Excitation-dependent photoluminescence maps for c) $(C_{60})_2$-CF_2 d) $(C_{60})_2$-$(CF_2)_2$ e) Bingel derivative of $(C_{60})_2$-CF_2. f) Bingel derivative of $(C_{60})_2$-$(CF_2)_2$. Concentration: 0.025 mg/ml.

In Fig.3 and Fig. S6 we present the excitation-dependent PL maps for the red region under 470 and the PL spectra under 365 nm excitation. The particles as expected aggregate in solution, hence the data presented here are for an agglomeration of fullerenes as proven by Dynamic Light Scattering. Dynamic Light Scattering measurements, indicated a formation of an aggregate consisting of 8 fullerene dyads for a Bingel derivative (Fig. S7).

The dyads exhibit similar emission patterns with a quantum yield of 2 % for the $(C_{60})_2$-CF_2 and 14 % for $(C_{60})_2$-$(CF_2)_2$ using pyrene as standard. These high quantum yields closely resemble carbogenic quantum dots which are synthesized in the range of 2-20 nm and have an emission maximum in the range of 430-480 nm with an optimum excitation range: 320-380 nm. [16] The fullerene $S_1 \rightarrow S_0$ transition appears at λ_{exc}=476 nm with λ_{em}=709 nm, while for the pristine C_{60} it is λ_{exc}=495 nm with λ_{em}=715 nm. This dual fluorescence is reminiscent of other ultra-small nanoscale carbon nanomaterials. The size of our materials is very close to the mean diameter of the dual fluorescent carbon dots reported by Zhou et al. [17] The second emission at 700-720 nm is coming from the fullerene core. Methods for making carbon dots include synthesis from chemical oxidation and ring opening of C_{60}, pyrolysis of small molecules and surface passivation of nano-graphite. [17-19] Chua et al reported the formation of highly fluorescent carbon dots by fullerene fragmentation through acid treatment and they called them graphene quantum dots. However, since fullerene contains a pentagon ring, these clusters cannot be considered as analogues of graphene. [18] The corannulene moiety with an isolated pentagon ring surrounded with hexagons is the core of the fullerene and upon surface functionalization it is fluorescent with 57 % QY; a value 8 times higher than of the parent corannulene. [20] Furthermore, fluorinated conjugated systems have lower HOMO-LUMO and bright electrogenerated chemiluminescence [9] with a series of perfluorinated compounds behaving as n-type semiconductors with blue emissions and QY value of 68 %. In general, the electronegative fluorinated groups have been considered to lower the HOMO-LUMO levels and to open the HOMO-LUMO gap compared to non-fluorinated polymers with similar backbones. [9] The dominant red emission after green excitation in pristine fullerenes arises from the fivefold degenerate h_{1u} to the three-fold degenerate t_{1u}. In order to clarify the presence of aggregation dependent optical properties, we recorded the PL spectra in different concentrations (Fig. S6). No spectral differences where observed over a broad concentration range.

An important application of fullerenes is their use as photosensitizers with regard to the very high yield of the reactive singlet oxygen state, generated through an energy transfer from their triplet state to oxygen. However, singlet oxygen can be detrimental to other biomedical applications due to its high reactivity and toxicity. The formation of an intermediate between the photosensitizer, that is subsequently deactivated, results in a phosphorescence at 1270 nm corresponding to the $O_2(^1\Delta_g) \rightarrow O_2(^3\Sigma_g^-)$ decay. We recorded the NIR emission of C_{60} and the dimers in CS_2, since toluene is quenching the singlet oxygen due to formation of toluene radicals. The Bingel $(C_{60})_2$-CF_2 is showing a weak photosensitization (Fig. 4), while for the Bingel derivative of $(C_{60})_2$-$(CF_2)_2$ the singlet oxygen phosphorescence is almost completely absent (see Fig.S8) following the same trend with the QY (Fig.4c). Notice that for the optimum singlet oxygen generation, the λ_{exc}=400 nm for the $(C_{60})_2$-$(CF_2)_2$ is significantly blue shifted compared to pristine C_{60} (λ_{exc}=550 nm, see Ref.22). Fullerenes have a notoriously weak fluorescence, due to the intersystem crossing that leads to a long lived and weak decay from T_1 to the S_0 state and a subsequent energy transfer to oxygen. As such, there is an unambiguous correlation between the increased fluorescence quantum yields and the singlet oxygen generation. Since this photocycle is suppressed, the predominant transition is radiative relaxation from S_1 to the ground S_0 and results to the high quantum yield. Similar suppression of the singlet oxygen generation has been previously observed in fullerenes functionalized with electronegative oxygen, for example $C_{60}O_3$, $C_{60}O_4$, $C_{60}O_5$ [21] and dyads with pyrene. [22]

In order to elucidate the differences between the photophysical properties of these new dimers and conventional fullerenes, we functionalized C_{60} with the same malonate unit (Fig.S9). The photosensitization efficiency of the malonates with two CF_2 bridging groups (Fig. 4) was tested and compared with the behavior of a C_{60} functionalized with one malonate unit. The singlet oxygen generation is weaker in the dyads signaling a quenching through the predominant S_0-S_1 transition. The optimum is λ_{exc} =473 nm for the Bingel (C_{60})-CF_2 with a weaker feature at 550 nm and at 400 nm for the $(C_{60})_2$-$(CF_2)_2$. For the pristine C_{60} the optimum λ_{exc} is 550 and 600 nm, significantly red

shifted. [22] Both the pristine dyad, (C_{60})-CF_2, and the malonate (C_{60})-$(CF_2)_2$, exhibit a biexponential decay time resolved fluorescence with one long and one short lifetime component (Fig. 4b). The lifetimes derived from the bi exponential decays are 0.53;2.85 ns for 420 nm, 0.73;3.24 ns for 440 nm, 0.84;3.58 ns; for 460 nm, 1;4 ns for 480 nm.
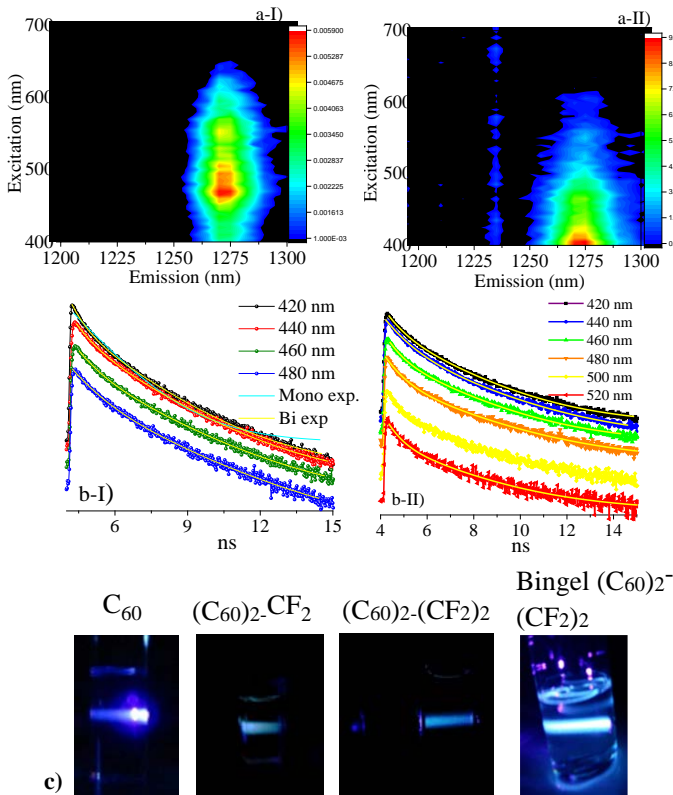

Figure 4. a) NIR PL for the (I) Bingel $(C_{60})_2$-(CF_2) (0.03 mg/ml in CS_2) and (II) the $(C_{60})_2$-$(CF_2)_2$. b) Time resolved fluorescence lifetime measurements. (I) Bingel $(C_{60})_2$-(CF_2) and (II) $(C_{60})_2$-CF_2. The fitting curves are shown in yellow lines. c) the illuminations of the samples with 400 nm light. From left to right: C_{60}, $(C_{60})_2$-CF_2, $(C_{60})_2$-$(CF_2)_2$, Bingel $(C_{60})_2$-$(CF_2)_2$.

In summary, two novel C_{60} dyads bridged with the electron withdrawing -CF_2- can be synthesized through an arc-discharge procedure. The structure of the dimers has been determined by ^{19}F NMR, ^{13}C NMR, mass spec and Raman/FTIR. HPLC analysis, shows that the addition of Teflon alters the thermodynamics of the systems, suppresses specific classes of fullerenes and stabilizes these unusual dyads. Detailed fluorescence studies indicated the similarity of their optical transitions compared to pristine and malonate C_{60}, resulting in reduced intensity of the singlet oxygen generation compared to conventional fullerenes. Malonate derivatives exhibited similar optical properties albeit with a more pronounced singlet oxygen sensitization. These materials represent a new class of carbon nanostructures that combine the versatile surface functionality of fullerenes with the photoluminescence properties of carbogenic dots.

Experimental Section

Graphite rods were vaporized in an arc-discharge reactor where Teflon tubes have been added. The arc-discharge took place under 80 mbar of constant helium flow and a dc current of 500 amps. The carbon soot was Soxhlet extracted with toluene. Bingel reaction: 0.05 mg of the $(C_{60})_2$-(CF_2) were dissolved in 0.1 ml of CS_2. Solutions of 1,8-Diazabicyclo[5.4.0]undec-7-ene (DBU) and diethyl bromomalonate were prepared accordingly: 0.005 ml of DBU in 4.995 ml toluene and 0.0057 ml diethyl malonate in 4.994 ml toluene. 0.005 ml of the DBU solution and 0.005 ml of the malonate solution were added in the fullerene solution. Further 0.01 and 0.0114 ml of the DBU and malonate solutions were added, the same after 2 hours, and 0.02+0.02 ml were finally added after $4^{1/2}$ hours. A C_{60} monomer functionalized with the same malonate unit was synthesized through 1:1:1 C_{60}: DBU: bromomalonate molar ratio.

References

1. J.L.Segura, N.Martin. *Chem. Soc. Rev.* **2000**, *29*, 13
2. R.Taylor, M.P.Barrow, T. Drewello, *Chem. Commun.* **1998**, 2497
3. K.Komatsu, G.W.Wang, Y.Murata, T.Tanaka, K.Fujiwara *J.Org.Chem.* **1998**, 63, 9358-9366
4. M.A. Lebedeva, T.W. Chamberlain, E. S.Davies et al *Beilstein J. Org. Chem.* **2014**, 10, 332–343
5. A.Gromov, S.Lebedkin, S.Ballenweg, A.G. Avent, R.Taylor, W.Kratschmer. *Chem. Commun.* **1997,** 209
6. J.Zhang, K.Porfyrakis, J.J.L.Morton, M.R.Sambrook, J.Harmer, L.Xiao, A. Ardavan, G.A.D. Briggs. *J.Phys.Chem.C.Lett.* **2008**, *112*, 2802-2804
7. S.Erten-Ela, C.Villegas, J.L.Delgado et al. *Science*, **1996**, *271*, 1833
8. Y. Rio, D. Sanchez-García, W. Seitz, T. Torres, J. L. Sessler, D. M. Guldi. *Chem.Eur. J.* **2009**, *15*, 3956;
9. U. Giovanella, C. Botta, F. Galeotti, B. Vercelli, S. Battiato, M. Pasini. *J. Mater. Chem. C.* **2013**, *1*, 5322–5329
10. Z.Wang, Y.Nakanishi, S.Noda, H.Niwa, J.Zhang, R.Kitaura, H.Shinohara. *Angew.Chem.Int.Ed.* **2013**, *52*, 11770
11. I.E. Kareev, I.V. Kuvychko, S.F. Lebedkin et al**.** *J.Am.Chem.Soc.* **2005**, *127*, 8362-8375
12. G-W.Wnag, K.Komatsu, Y.Murata, M.Shiro. *Nature* **1997**, *387*, 583.
13. H.Kuzmany, R.Pfeiffer, M.Hulman, C.Kramberger. *Phil.Trans.R.Soc.Lond. A.* **2004**, *362*, 2375
14. Z.Wang, Y.Nakanishi, S.Noda, K.Akiyama, H.Shinohara. *J.Phys.Chem.C.* **2012**, *116*, 25563-25567
15. V Filidou, S Simmons, SD. Karlen, F Giustino, HL. Anderson, JJ.L. Morton. *Nat.Phys.* **2012**, *8*, 596
16. M.J.Krysmann, A.Kelarakis, P.Dallas, E.P.Giannelis. *J.Am.Chem.Soc.* **2012**, *134*, 747
17. W.Zhou, J.Zhuang, W.Li, C.Hu, B.Lei, Y.Liu. *J. Mater. Chem. C*, **2017**, *5*, 8014--8021
18. C.K.Chua, Z.Sofer, P.Simek, O.Jankovsky, K.Klımova, S. Bakardjieva, S.H.Kuckova, M.Pumera *ACS Nano* **2015**, *9*, 2548
19. N.Fuyuno, D.Kozawa, Y.Miyauchi, S. et al. *Adv.Optical Mater.* **2014**, *2*, 983-989

20. J.Mack, P.Vogel, D.Jones, N.Kavala, A.Sutton. *Org. Biomol. Chem.*, **2007**, *5*, 2448–2452

21. T.Hamano, K.Okuda, T.Mashino, M.Hirobe, K.Arakane, A.Ryu, S.Mashikoc, T.Nagano. *Chem.Commun.* **1997**, 21

22. P.Dallas, G.Rogers. B.Reid, R.Taylor, H.Shinohara, G.A.D.Briggs, K.Porfyrakis. *Chem.Phys.* **2016**, *465-466*, 28-29

Text for Table of Contents
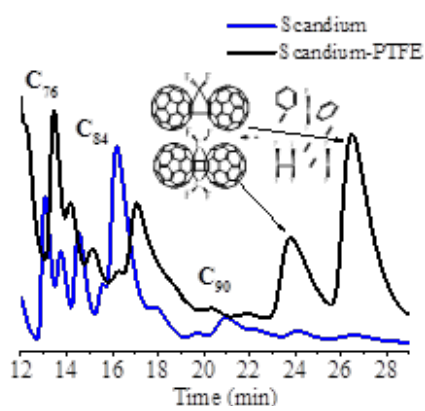
*Panagiotis Dallas *[a], Shen Zhou [a], Stuart Cornes [a], Hiroyuki Niwa [b], Yusuke Nakanishi [b], Yasuhiro Kino [b], G.Andrew.D.Briggs [a], Hisanori Shinohara *[b] and Kyriakos Porfyrakis *[a]*

Page No. – Page No.

–CF$_2$- bridged C$_{60}$ dimers and their optical transitions